ACI STRUCTURAL JOURNAL TECHNICAL PAPER

Title no. 84-S51

Nonlinear Analysis of Reinforced Concrete Frames Subjected to Thermal and Mechanical Loads

by Frank J. Vecchio

A simple analytical procedure is presented that enables accurate prediction of the response of reinforced concrete plane frames to thermal and mechanical loads. The formulations given allow standard linear elastic procedures to be used in a nonlinear mode by incorporating secant stiffness factors and an iterative solution process. Rigorous section analyses, using a layered approach, are performed in determining effective member stiffnesses. Influencing factors such as nonlinear material stress-strain response, tension stiffening effects, membrane action, thermal creep, load and time history, nonlinear thermal gradients, and material properties at elevated temperatures can be taken into account using appropriate models. Preliminary test results are compared to predictions obtained from the proposed procedure, and good agreement is obtained. Aspects pertaining to the application and performance of the method are also discussed.

Keywords: frames; loads (forces); reinforced concrete; stiffness; stress-strain relationships; **structural analysis;** tension; tests; thermal gradient; **thermal stresses.**

Many reinforced concrete structures are exposed to thermal loadings, whether through design or as a consequence of unavoidable conditions. These thermal loads can be the result of ambient conditions, heat of hydration, service function, or fire (see Fig. 1). They can, in some instances, represent the most critical loading condition[1,2] and must be expressly considered in the design of the structure.

A reinforced concrete structure subjected to thermal loads will develop stresses as a result of restrained thermal expansion. In continuous structures, two components of thermal stress can be identified: primary thermal stresses and continuity thermal stresses.[1] Primary thermal stresses are induced in a section where a nonlinear thermal gradient exists. Self-equilibrating across the section, they arise from the incompatibility between the two requirements that plane sections remain plane and that unstressed fibers expand by an amount proportional to the local temperature rise [see Fig. 2(a)]. Continuity thermal stresses, on the other hand, are the stresses induced in indeterminate structures as the result of restrained member deflections and rotations arising from thermal deformations [see Fig. 2(b)]. In most instances, continuity thermal stresses are of greater magnitude than primary thermal stresses and play the major role in causing structural distress.[3]

The thermal stresses induced in reinforced concrete structures are unlike most other mechanical stresses in that they tend to be self-relieving to some extent. The

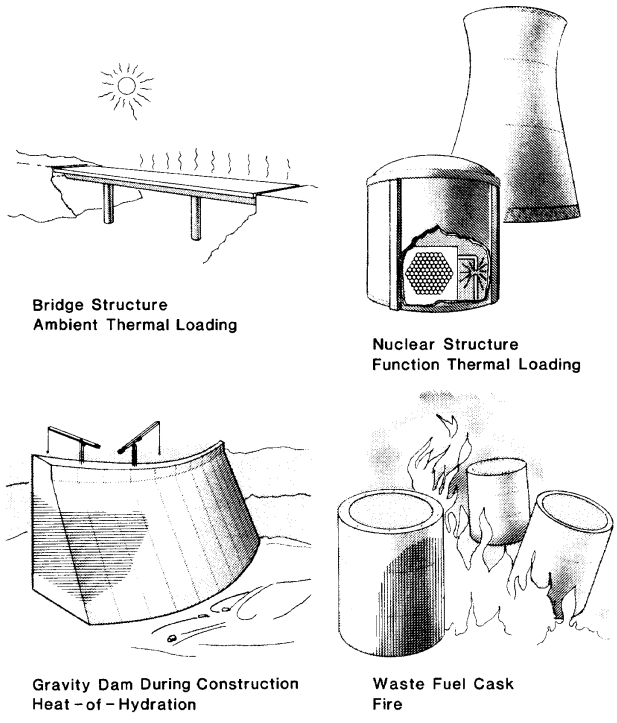

Fig. 1 — Types of thermal loads and example situations

Received Aug. 6, 1986, and reviewed under Institute publication policies.

*ACI member **Frank J. Vecchio** is an assistant professor in the Department of Civil Engineering at the University of Toronto. Prior to joining the university, he was a structural research engineer with Ontario Hydro where he was involved in research related to the analysis and design of reinforced concrete nuclear power plant structures. He is a member of ACI Committee 435, Deflection of Concrete Building Structures.*

magnitude of thermal stress induced is, in part, governed by the effective stiffness of the member. As cracks develop and propagate within the concrete, the effective stiffness of the member is reduced, thus causing a relaxation in the thermal bending moments. Because of this characteristic, conventional methods of structural analysis are not directly applicable to thermal loadings. However, various alternative methods of analysis have been proposed; these will be reviewed briefly.

Analytical methods for determining primary thermal stresses in a reinforced concrete section are well established. Priestley[4] developed a closed-form solution for a general uncracked isotropic homogeneous section subjected to an arbitrary vertical temperature distribution. He found excellent agreement between theory and experimental results from a quarter-scale model of a box-girder bridge. Thurston[3] modified the theory such that it enabled the analysis of cracked sections. He too was able to obtain excellent agreement between theory and experimental results. Alternative methods have been described by Freskakis[5] and Pajuhesh.[6] In general, all of the methods are reasonably simple and fundamentally sound. They are not restricted by a need for simplifying assumptions regarding tensile strength, temperature distributions, or other behavioral characteristics.

Various analytical methods have also been proposed for the analysis of continuity thermal stresses in reinforced concrete frame structures. The methods proposed by Mentes, Bhat, and Ranni,[7] Thurston,[3] Kar,[8] ACI Committee 349,[9] and Gurfinkel[10] are among the more accepted procedures. In general, these analytical methods attempt to account for reduced member stiffness when determining moment distributions within a thermally loaded frame. However, owing to the complexity of the problem, the methods tend to be complicated and/or rely on simplifying assumptions. Many do not adequately account for such factors as concrete tension, tension-stiffening effects after cracking, mechanical load interactions, nonlinear thermal gradients, or nonuniformly cracked members. Any one of these factors may severely compromise the ability to make accurate predictions in some cases. Not surprising, the methods yield radically differing results.[11] Apart from Thurston's, which appears to be the more rigorous and accurate as well as the most complex, little experimental data is provided to corroborate the proposed methods.

In this paper, an alternate computer-based procedure is presented for the analysis of reinforced concrete frames subjected to thermal loads. The method is not restricted by any particular set of simplifying assumptions. It is distinct from previously proposed methods

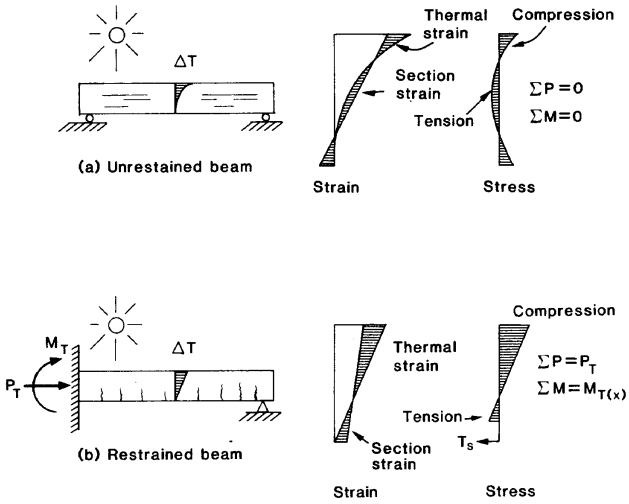

Fig. 2 — Types of thermal stresses: (a) primary thermal stress; (b) continuity thermal stress

in that it utilizes section analysis procedures that can take into account nonlinear material response and time- and temperature-dependent effects.

OVERVIEW OF PROPOSED ANALYTICAL PROCEDURE

The analytical procedure proposed essentially involves a total load, iterative, secant stiffness approach to nonlinear frame analysis. The computer-based method incorporates realistic constitutive relations for the concrete and reinforcement, and it allows for the consideration of thermal creep, nonlinear thermal gradients, and previous load history. The combined effects of both thermal and mechanical loadings can be analyzed, with the thermal load effects including both primary and continuity thermal stressing.

A linear elastic frame analysis is initially performed, using uncracked gross section properties, to determine a first estimate of the resultant internal member forces arising from the thermal and mechanical loads imposed. Each member, at various sections along its length, is then analyzed for its nonlinear sectional behavior in terms of axial force-elongation and moment-curvature response. Effective secant stiffness factors are determined from the section analyses. These stiffness factors are used first to reevaluate the fixed-end member forces arising from the imposed loads. Second, they are used to redefine the global stiffness matrix for the structure. A linear elastic reanalysis of the frame is performed using the modified stiffness factors and member end-actions, and revised force resultants are determined. The process is repeated, in an iterative manner, until all stiffness factors converge to constant values, at which point final forces, displacements, stresses, and strains can be computed.

A simplified flowchart for the procedure is given in Fig. 3. A preliminary computer code based on this procedure, program TEMPEST, is documented in Reference 12. The elastic plane frame analysis routine used as a basis for the procedure is that described by Gere and Weaver in Reference 13.

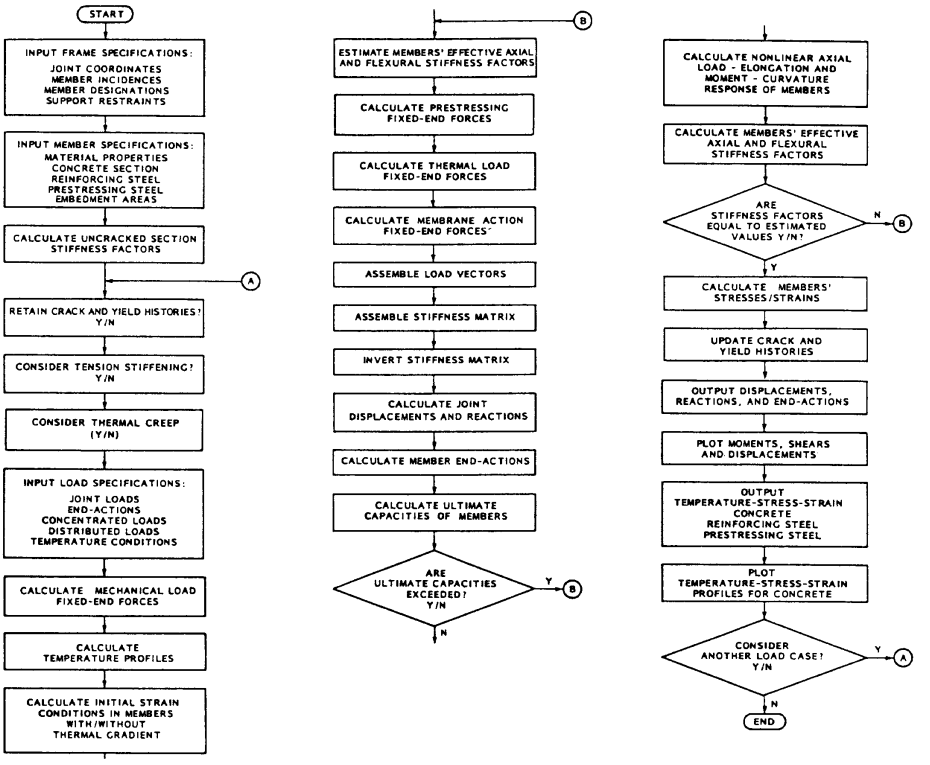

Fig. 3 — Algorithm for proposed analytical procedure

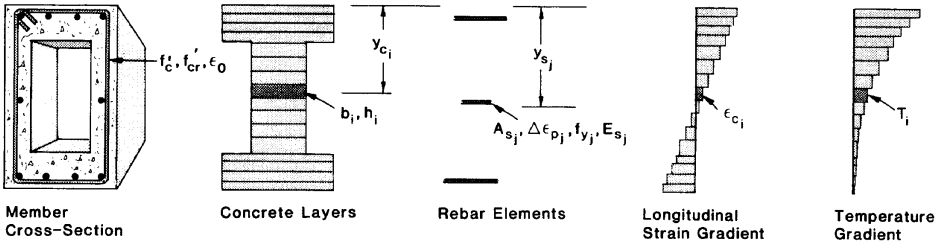

Fig. 4 — Variables in a layered section analysis

SECTION ANALYSIS

Response of each reinforced or prestressed concrete section to thermal and mechanical loads is determined using a layered analysis. In this method, the section is discretized into a number of concrete layers, reinforcing bar elements, and prestressing steel elements, and each is analyzed separately (see Fig. 4). Temperature, strain, and stress are determined at the middepth of each component, and a numerical integration of the resulting moments and forces is then performed. The analysis employs a convergence procedure satisfying the criteria that plane sections remain plane and that equilibrium of forces be maintained across the section. The solution algorithm used is summarized in the Appendix.

The plane section hypothesis permits the calculation of longitudinal strain in each element of concrete, reinforcing steel, and prestressing steel as a function of the top and the bottom fiber strains. Stresses in these components are then calculated from the longitudinal strains using appropriate constitutive relations. The effects of shear and transverse strains are ignored. Estimates of the top fiber strain and the bottom fiber strain are adjusted until the following two equilibrium conditions are met

$$P = \sum_{i=1}^{m} f_{ci} \cdot b_i \cdot h_i \cdot + \sum_{i=1}^{n} f_{si} \cdot A_{si} \tag{1}$$

$$M = \sum_{i=1}^{m} - f_{ci} \cdot b_i \cdot h_i \cdot (\bar{y} - y_{ci}) + \sum_{i=1}^{n} - f_{si} \cdot A_{si} \cdot (\bar{y} - y_{si}) \tag{2}$$

where

m, n = number of concrete layers and reinforcing bar elements, respectively
b, h = width and depth of a concrete layer
A_s = cross-sectional area of reinforcing steel
y_c = distance from top fiber to center of concrete element
y_s = distance from the top fiber to center of reinforcing steel element

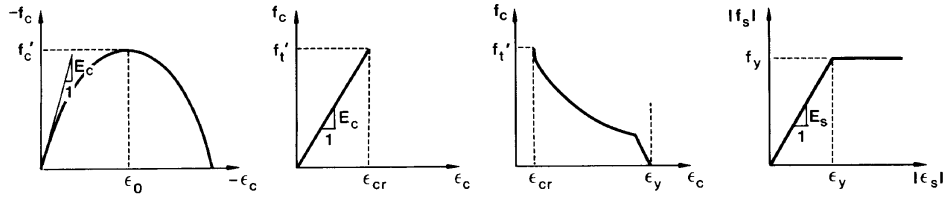

(a) Concrete in Compression

(b) Concrete Tension Prior to Cracking

(c) Concrete Tension Post-Cracking

(d) Reinforcing Steel

Fig. 5 — Constitutive relations for concrete and reinforcement

$\bar{y}$ = distance from top fiber to centroid of section
f_c = stresses in the concrete
f_s = stresses in the reinforcing steel
M = moment acting on the section
P = axial load on the section

In analyzing a member's response to load, a compatible strain condition is sought that will satisfy section equilibrium according to the governing constitutive relations. The relations currently used account well for the nonlinear response of reinforced concrete.

The constitutive relation for concrete in compression, shown in Fig. 5(a), is the simple parabolic expression proposed by Hognestad, as follows

$$f_c = -f_c' \left[2\left(\frac{\epsilon_c}{\epsilon_o}\right) - \left(\frac{\epsilon_c}{\epsilon_o}\right)^2 \right] \tag{3}$$

where
ϵ_c = strain in the concrete
ϵ_o = strain at maximum compressive stress ($\simeq -0.002$)
f_c = stress in the concrete
f_c' = maximum compressive stress

Note that the concrete strain ϵ_c is that portion of the total strain that causes stress. Thermal strain and creep strains are subtracted from the total strain to determine ϵ_c.

For concrete in tension [Fig. 5(b)], where the concrete strain does not exceed the tensile cracking strain, the concrete tensile stress is computed from the following relations

$$f_c = E_c \cdot \epsilon_c; \qquad 0 \leqslant \epsilon_c \leqslant \epsilon_{cr} \tag{4}$$

$$\epsilon_{cr} = \frac{f_{cr}}{E_c} \tag{5}$$

$$E_c = \frac{2f_c'}{\epsilon_o} \tag{6}$$

where
ϵ_{cr} = cracking strain
E_c = modulus of elasticity
f_{cr} = tensile cracking strength of concrete

If the concrete strain exceeds the cracking strain and tension stiffening effects are ignored, then the concrete tensile stress is taken as zero. However, in the normal case where tension stiffening effects are considered, the constitutive model[14] utilized is

$$f_c = f_{cr} \cdot \frac{1}{1 + \sqrt{200\,\epsilon_c}} \tag{7}$$

subject to the condition that combined concrete and steel tensile forces do not exceed the steel yield force [see Fig. 5(c)].

Post-cracking tensile stresses are assumed to exist only in that area of concrete that is defined as the effective embedment region for a reinforcing bar. This region should not exceed the area of a square whose sides are 7.5 times the reinforcing bar diameter. Reductions in the area due to overlapping embedments and proximity to edges of the section must be taken into account.

For reinforcing steel, a bilinear stress-strain relationship is employed as shown in Fig. 5(d), and perfect bond between the reinforcement and the concrete is assumed. Strain-hardening effects are ignored. Thus, the constitutive relations are as follows

$$f_s = E_s \cdot \epsilon_s; \; |f_s| < f_y \tag{8}$$

$$\epsilon_s = \epsilon_c \tag{9}$$

where
ϵ_s = strain in the reinforcement
E_s = modulus of elasticity of steel
f_s = stress in the reinforcement
f_y = yield stress of the reinforcement

Similar relations are used for prestressing steel components, except that the locked-in prestressing strain $\Delta\epsilon_p$ is taken into account as described in Eq. (10)

$$\epsilon_s = \epsilon_c + \Delta\epsilon_p \tag{10}$$

Strength, stiffness, and other physical properties of concrete and of reinforcing steel are significantly affected at elevated temperatures. Hence, the analytical procedure is structured to take strength-temperature dependence into account when determining a section's

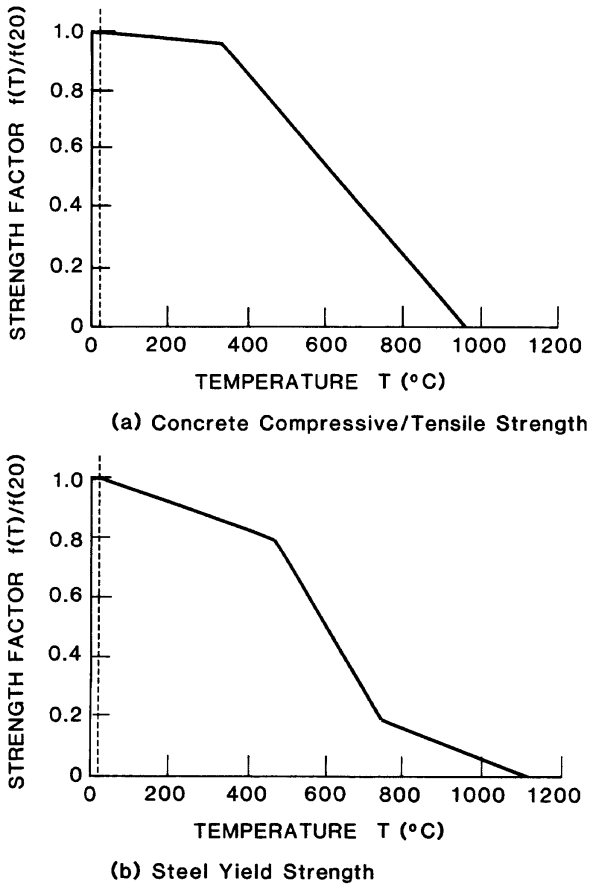

Fig. 6 — Material properties at elevated temperatures

response to load. The exact nature of the influence is much debated and still in need of further research. The relationships currently employed are depicted in Fig. 6.

For members under thermal load, nonlinear transient temperature profiles are determined using standard one-dimensional heat flow principles. The temperature at the mid-depth of each concrete, reinforcing bar, and prestressing steel component of the section is determined using the following governing equation

$$T_i = T_1 + (T_2 - T_1)\, x/H + \frac{2}{\pi}\sum_{n=1}^{\infty} \times \left(\left\{ \frac{[T_2 \cos(n\pi) - T_1] - [T_2' \cos(n\pi) - T_1']}{n} \right\} \times \sin\left(\frac{n\pi x}{H}\right) \exp\left(\frac{-kn^2\pi^2 t}{H^2}\right) \right) \quad (11)$$

H = depth of the member
x = distance from the bottom surface to midpoint of element i
T_i = temperature at midpoint of element i
T_1 = temperature at the bottom surface
T_2 = temperature at the top surface
T_1' = initial temperature at the bottom surface
T_2' = initial temperature at the top surface
t = elapsed time
k = thermal diffusivity of concrete

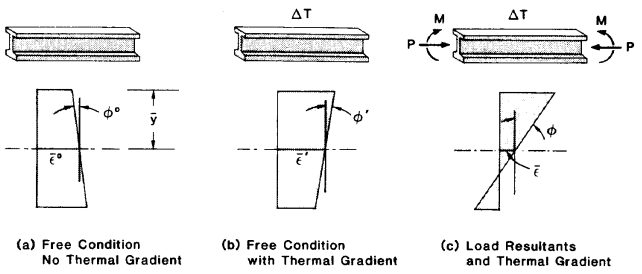

Fig. 7 — Strain conditions used in calculating effective stiffness factors and fixed-end forces

EFFECTIVE STIFFNESS FACTORS AND FIXED-END FORCES

Secant stiffness factors are evaluated for a given member under a specific load condition by examining that member's cross-sectional strains both with and without the loads acting. Strain conditions are determined by considering the equilibrium and compatibility requirements discussed previously.

Fig. 7 illustrates the strain values used in computing member stiffness factors. Under the action of thermal load ΔT, axial load P, and end moment M, the section's centroidal fiber strain is $\bar{\epsilon}$ and the curvature is ϕ. Under thermal load alone, the centroidal fiber strain and the curvature are $\bar{\epsilon}'$ and ϕ', respectively. Given these values, the effective stiffness factors are evaluated using the following relations

$$A_e = \frac{P}{E_c \cdot (\bar{\epsilon} - \bar{\epsilon}')} \quad (12)$$

and

$$I_e = \frac{M}{E_c \cdot (\phi - \phi')} \quad (13)$$

where
A_e = effective axial stiffness
I_e = effective flexural stiffness
E_c = modulus of elasticity of concrete [from Eq. (6)]

It is recognized that the two factors are not completely independent, but that $\bar{\epsilon}$ is affected by the moment M and that ϕ is affected by the axial load P. However, this is not a concern since the two factors, when used together, will return the correct values for top and bottom fiber strains and thus represent the true strain conditions in the members. This would not be acceptable if an incremental load and tangent stiffness approach were being used.

In most elastic frame analysis programs, fixed-end forces are determined solely from the magnitude of the applied loads and from the lengths of the members on which they act. The fixed-end forces are then used to define a load vector, as discussed in Reference 13. A global stiffness matrix is assembled and inverted, and final deflections and force distributions are then calculated directly. Unfortunately, this direct method cannot be used for a nonlinear thermal load analysis.

Thermal fixed-end forces depend greatly on the effective stiffnesses of the members; as stiffnesses change, so should the thermal fixed-end forces. Thus, it is necessary to reevaluate thermal load fixed-end forces during each iteration of the solution process.

The relations used to determine these forces are also illustrated in Fig. 7. Having calculated effective stiffness factors for a member at a particular load level, the thermal load fixed-end forces are checked by examining initial strain and free thermal strain conditions. If the member's initial centroid fiber strain and curvature are $\bar{\epsilon}^\circ$ and ϕ°, and if under free thermal load the strain conditions are $\bar{\epsilon}'$ and ϕ', then the fixed-end forces are determined by the following relations

$$P_{ft} = A_e \cdot E_c \cdot (\bar{\epsilon}' - \bar{\epsilon}^\circ) \tag{14}$$

and

$$M_{ft} = I_e \cdot E_c \cdot (\phi' - \phi^\circ) \tag{15}$$

where

P_{ft} = fixed end axial force due to thermal load
M_{ft} = fixed-end moment due to thermal load

Note that $\bar{\epsilon}^\circ$ and ϕ° will be equal to zero if the member is not prestressed.

Member end-actions for prestressing loads are determined in a similar manner. Given the section strain conditions ϵ° and ϕ° under free conditions, the prestressed fixed-end forces are

$$P_{fp} = A_e \cdot E_c \cdot \bar{\epsilon}^\circ \tag{16}$$

$$M_{fp} = I_e \cdot E_c \cdot \phi^\circ \tag{17}$$

where

P_{fp} = fixed end axial force due to prestressing
M_{fp} = fixed-end moment due to prestressing

Again, these actions must be reevaluated during each iteration because of the changing member stiffnesses.

To insure that axial strain compatibility is maintained — essential to a proper account of membrane action — the concept of fixed-end forces is again utilized. These forces are made to attain the values required to insure that the total axial elongation in a member, determined from a summation of the average axial strain over the length of the member, matches the elongation determined from the end-joint deflections. Thus

$$P_{fm} = P'_{fm} + E_c \cdot A_e \cdot (\bar{\epsilon} - \Delta/L) \tag{18}$$

where

P_{fm} = fixed end axial force due to membrane action
P'_{fm} = fixed end axial force due to membrane action determined from the previous iteration
Δ = relative deflection of the member end-joints in the longitudinal direction
L = length of member

It should be noted that the average axial strain $\bar{\epsilon}$ is determined from a rigorous section analysis as previously described. Also note that the force P_{fm} is a correction term meant to overcome any errors introduced by limitations placed on the effective stiffness A_e (e.g., in some situations A_e could be computed as being negative, which is not permitted). In most situations, the force P_{fm} will be of value close to zero.

ADDITIONAL FEATURES AND CONSIDERATIONS

The primary advantage of the proposed method is in its ability to perform rigorous analyses of reinforced concrete members under thermal load by simple modification of standard linear elastic frame analysis procedures. The stress-strain relationships currently employed are more realistic than those utilized in most other procedures, with the tension stiffening aspects being perhaps the most crucial towards accurately predicting response. As improved constitutive relations are developed, they may be incorporated into the procedure without difficulty. This is also true of mathematical models for thermal creep and for changes in the physical and mechanical properties of the materials at elevated temperatures. Because sectional analyses are performed in determining effective stiffness factors, rather than relying on empirical formulation such as Branson's formula, it is possible to obtain complete stress, strain, and temperature profiles for members throughout the structure. This is in addition to the customary displacements, reactions, and member end-actions obtained from frame analyses. Also, it affords the ability to consider rigorously the combined effects of primary thermal stresses, continuity thermal stresses, prestressing, and mechanical loading simultaneously. Most of the procedures previously discussed are deficient in these respects.

The layered cross-sectional approach utilized allows for the precise definition of frame member cross sections, including specification of irregular section geometry and multipositioning of reinforcement and prestressing steel. Hybrid steel/concrete frames can also be treated. Notable, too, is the ability to consider time-dependent transient thermal load effects.

The cracking of concrete and yielding of reinforcement sustained by a structural member under previous loading will influence that member's response to newly applied loads. Or, in the case of thermal loading, the damage sustained shortly after the application of load will alter the member's long-term response. These factors are taken into consideration by retaining crack histories for each of the concrete layers and yield histories for each of the reinforcing bar elements of each member. The option of resetting uncracked and unyielding conditions at any time exists.

Once a concrete layer is cracked, it remains cracked regardless of the future strain conditions imposed. Direct tension cannot be sustained in a previously cracked layer although tension stiffening effects can be taken into account. In the event of compressive strain, the

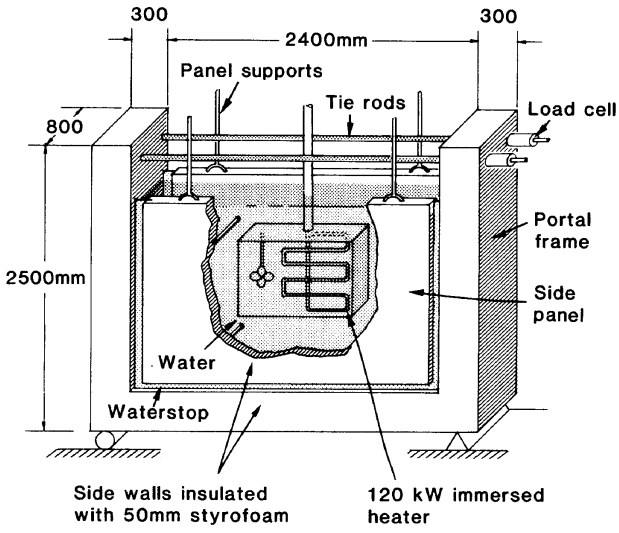

Fig. 8 — Schematic representation of test model PF1

crack is assumed to close but not heal, and direct compression is transmitted across the crack in the same manner as in an uncracked layer.

For reinforcing and prestressing steel, any strain beyond the yield point is retained as an offset strain. This offset is subtracted from the strain incurred during future load cases to determine the acting stress. The magnitude of the offset is redefined if further yielding occurs.

During each iteration of the solution procedure, internal member forces are reevaluated according to the effective stiffness factors determined from the previous iteration. This procedure is continued until all member stiffness factors converge to constant values. However, if the resultant forces determined for a particular member exceed that member's ultimate load capacity, then this solution procedure becomes unstable. Thus, it is necessary to check that all members can sustain the acting loads before an attempt is made to determine strain response. Given the axial load acting on a particular member, an ultimate moment capacity can be computed and checked against the acting moment. If the acting moment exceeds the moment capacity, the effective stiffness factors for that member are reduced to those computed at ultimate load. In the reanalysis that follows, if enough load is shed from the member in question (due to reduced stiffness) to bring the resulting moment to a level below the ultimate capacity, then the regular solution procedure is resumed. If the resulting moment still exceeds capacity, then failure of the structure is assumed to have occurred.

APPLICATION AND PERFORMANCE

Discussed in Reference 12 is a sample problem solved using a preliminary version of the procedure presented here. A comparison of the elastic and inelastic solutions is made in respect to force redistributions and increased deflections — both found to be significant. Considerations involved in applying the solution procedure, as well as the convergence characteristics of the procedure, are also described. Some general observations are reiterated here.

The analytical procedure requires that each frame member be broken down into one or more member segments. The greater the number of segments used, the greater the accuracy of the analysis since changes in stiffness along a member's length would be better taken into account. In general, the number of segments used per member should reflect the complexity of the moment pattern in that member. When a moment is relatively constant along the member's length, one or two segments will suffice. When the member is subjected to significantly varying moment from one end to the other, three or more segments should be used. Wherever possible, segment ends should correspond to peak-moment points and points of contraflexure. The number of segments used need not be the same for each member in the frame.

A further point to be made lies in the efficiency and convergence characteristics of the iterative procedure using secant stiffness factors. In the analysis of large frames, where length of computation time becomes a concern, efficiency in the process is essential. It has been found that, in most cases, no more than approximately 10 iterations are needed before convergence is attained to within 1 percent of the final results. Of course, there may be some unusual or ill-behaved structural systems where more iterations will be required or where user interaction will be necessary to achieve convergence.

EXPERIMENTAL VERIFICATION

An extensive experimental and analytical research program was recently undertaken at Ontario Hydro to study thermal gradient effects in reinforced concrete nuclear containment structures. Three large-scale portal frame models were to be tested under various thermal and mechanical loading conditions with the objective of obtaining data necessary to verify and refine the analytical procedure described. Testing of the first two models is complete, and the third is in progress. Full details and test results will be presented at the conclusion of the program. Some preliminary results from the first test will be examined here to obtain an indication of the accuracy of the theoretical analysis procedure.

A schematic representation of the first test model is shown in Fig. 8. The model is essentially a reinforced concrete portal frame consisting of two columns each 300 x 800 x 2350 mm (12 x 32 x 92 in.) and one beam 300 x 800 x 2200 mm (12 x 32 x 86 in.). The model sits in an inverted position with the ends of the columns connected by two 25 mm (1 in.) diameter tie rods. Spanning the interior of the frame to form a tank-like structure are two reinforced concrete side panels each 125 x 1500 x 2200 mm (5 x 60 x 86 in.). Flexible silicone waterstops bridge the gaps between the panels and the frame, allowing the frame to be structurally independent of the panels and thus unaffected in its stiffness or response. Water is placed in the tank to a depth

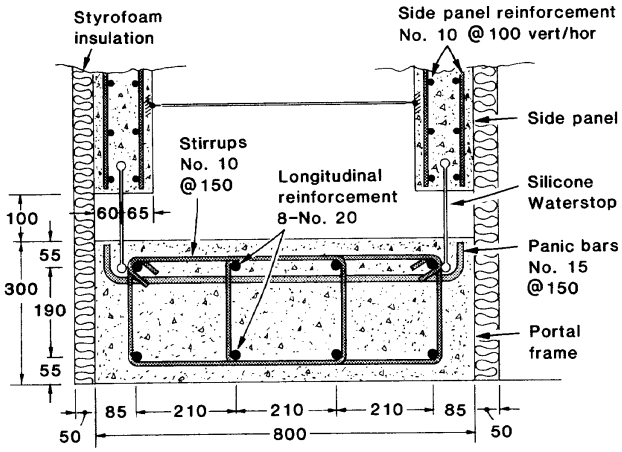

Fig. 9 — Details of model's member cross section

of 1500 mm (60 in.) and a 120-kW heater, immersed in the water, is used to apply thermal loads to the structure. The sides of the model are insulated to insure unidirectional heat flow from the inside surfaces to the outside surfaces of the frame. Mechanical loads can be applied simultaneously by pretensioning the tie rods. The test specimen is heavily instrumented with load cells, thermocouples, strain gages, and displacement transducers to monitor its reponse.

The beam and columns of the frame were equally reinforced with 1 percent total longitudinal reinforcement (four No. 20 bars, top and bottom; see Fig. 9). (In the second and third models, percentages of reinforcement in the members vary.) Shear reinforcement consisted of No. 10 bars spaced at 150-mm (6-in.) centers. The concrete used in casting the portal frame had a 42.4 MPa (6.50 ksi) compressive strength and a 3.12 MPa (450 psi) split-cylinder tensile strength. Modulus of elasticity was measured at 28,980 MPa (4200 ksi) and thermal diffusivity at 0.774 mm^2/sec (1.20 x 10^{-3} $in.^2$/sec). The effective coefficient of thermal expansion was 8.2 x 10^{-6}/C (4.56 x 10^{-6}/F), measured wet. For the longitudinal reinforcement, the yield strength and ultimate tensile strength of the bars were found to be 448 MPa (64.5 ksi) and 709 MPa (102.8 ksi), respectively, based on a nominal cross-sectional area of 314 mm^2 (0.49 $in.^2$). Modulus of elasticity was measured at 217,000 MPa (31,500 ksi) and coefficient of thermal expansion at 12.4 x 10^{-6}/C (6.89 x 10^{-6}/F).

A number of tests were conducted on the model under various loading and restraint conditions. The focus here, however, will be on the results of thermal "shock" tests where the inside temperature was brought up as quickly as possible to a predetermined level (heating rate was typically 1 C/min) while the column ends were completely restrained by the tie rods. Three series of shock tests were conducted, with the variable being the amount of pretension in the tie rods. For Shock Series I, the total preload was 3.1 kN (0.70 k). For Series II and III, the preloads were 22.9 kN (5.15 k) and 38.5 kN (8.65 k), respectively. In each series, the shock tests involved gradients ranging up to 80 C (176 F) (e.g., 98 C [208 F] inside temperature,

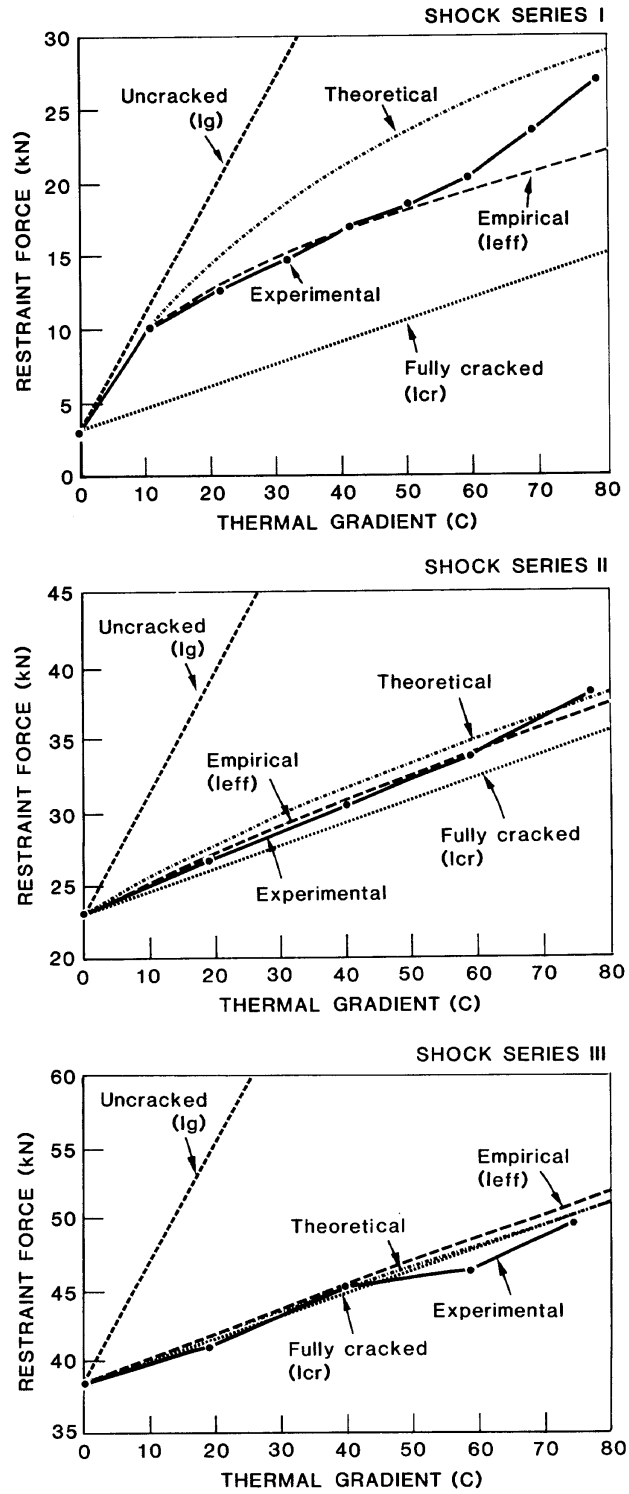

Fig. 10 — Summary of "shock series" test results together with predicted responses

18 C [64 F] outside temperature). Each test represented a more severe condition than the previous so that the effects of previous loading could be minimized. Of prime interest was the magnitude of restraint force that would be induced at various temperature levels.

Shown in Fig. 10 are the restraint forces induced at the columns as a result of thermal gradients applied to the test specimen for Shock Series I, II, and III. Also shown are the values predicted by four alternate meth-

ods of analysis. Note that the lever arm to the center line of the beam is 2.05 m (80.7 in.), that the cracking and yield moments of the beam section are 29 kN-m (21.4 ft-kip) and 125 kN-m (92.2 ft-kip), and that a moment of 9.1 kN-m (6.7 ft-kip) acts at the beam mid-span due to water and self-weight.

The "fully cracked sections" methods of analysis suggested by Gurfinkel,[10] Pajuhesh,[6] and others assume that the entire tensile region of a member is fully cracked in all load cases. For frame analyses, all members assume stiffnesses equal to their cracked moment of inertia I_{cr}. As can be seen in Fig. 10, this procedure greatly underestimates the forces measured in the test structure during Shock Series I, where relatively low levels of mechanical loads were acting. In Shock Series II and III, with higher levels of load acting, response is closer to that of the fully cracked assumption.

The method suggested by ACI Committee 349[9] recognizes that uncracked lengths might exist in a member near the regions of contraflexure. The cracked and uncracked regions are determined on the basis of mechanical moments alone, and thermal moment distribution is carried out considering this variation in stiffness along the member. For the test specimen, which was uncracked under mechanical loads alone for Shock Series I tests, the method implies that the uncracked or gross moments of inertia be used. This results in greatly overestimated restraint forces.

The "effective stiffness" methods proposed by Mentes, Bhat, and Ranni[7] and Thurston[3] assume that the effect of cracked and uncracked lengths in a member is equivalent to an effective moment of inertia given by Branson's formula, i.e.

$$I_e = \left(\frac{M_{cr}}{M_a}\right)^3 \cdot I_g + \left[1 - \left(\frac{M_{cr}}{M_a}\right)^3\right] \cdot I_{cr} \qquad (19)$$

With this relationship, standard methods of frame analysis can be used in an iterative procedure to solve for acting forces. As can be seen from Fig. 10, the method predicts well the experimental results, although the tendency is to underestimate slightly at higher thermal load levels during Shock Series I.

Also shown is the predicted response obtained using the analytical procedure described in this paper. It too predicts well the experimental results. The overestimation of force in the 20 to 30 C (68 to 86 F) range of Series I is likely related to the fact that the structure was precracked slightly from previous testing. The overall tendency to overpredict slightly the response is primarily related to two factors: (1) The constitutive relation used to model tension-stiffening effect [i.e., Eq. (7)] appears to overpredict strength in flexural members. An improved formulation is required. (2) Thermal creep, which was not taken into account in the theoretical model, was manifested in the experimental results; thermal creep resulted in significant reductions in restraint force over time durations as short as 12 hr.

CONCLUSIONS

A computer-based nonlinear frame analysis procedure, based on a secant stiffness formulation and an iterative analysis approach, was developed. The procedure can be used to predict accurately the response of reinforced concrete structures to thermal and/or mechanical loads. Rigorous section analyses of members are performed, utilizing realistic constitutive relations for concrete and reinforcement, in determining effective stiffness factors. The general procedure and specific formulations presented can be incorporated into most linear elastic frame analysis programs.

The advantage of the proposed procedure over other methods is in its ability to consider a wide range of influencing factors. Models for nonlinear stress-strain response of concrete and reinforcement, nonlinear thermal gradients, thermal creep, time history, load history, changes in material properties at elevated temperatures, and irregular section geometries have been implemented. Improved formulations, as they become available, can be incorporated without difficulty. Also, interactive effects between primary thermal stresses, continuity thermal stresses, and mechanical loads are inherently considered.

Experimental results show that the procedure yields fairly accurate predictions, although the tendency is to overpredict the response somewhat. An improved formulation for tension-stiffening effect and the inclusion of a model for thermal creep effect are seen as the essential factors in obtaining still better accuracy. Current work is in this direction.

ACKNOWLEDGMENTS

The experimental work and preliminary formulation of the analytical procedure were conducted at and funded by Ontario Hydro. Further development of the procedure was undertaken at the University of Toronto, under a grant from the Natural Sciences and Engineering Research Council of Canada. The author would like to express his gratitude for this support.

NOTATION

A_e = effective cross-sectional area of member
A_s = cross-sectional area of reinforcing steel
b = width of concrete layer
E_c = modulus of elasticity of the concrete
E_s = modulus of elasticity of the reinforcing steel
f_c = stress in the concrete
f'_c = concrete compressive strength
f_{cr} = concrete cracking strength
f_s = stress in the reinforcing steel
f_y = yield stress of the reinforcing steel
h = depth of concrete layer
H = total depth of member cross section
I_{cr} = cracked moment of inertia of member
I_e = effective moment of inertia
I_g = gross moment of inertia
k = thermal diffusivity of concrete
L = length of member
m = number of concrete layers in member cross section
M = moment acting at member section
M_a = maximum moment acting on member
M_{cr} = cracking moment for member
M_{fp} = fixed-end moment due to prestressing
M_{ft} = fixed-end moment due to thermal load

n = number of reinforcing bar elements in member cross section
P = axial force acting at member section
P_{fm} = fixed-end axial force due to membrane action
P_{fp} = fixed-end axial force due to prestressing
P_{ft} = fixed-end axial force due to thermal load
t = elapsed time
T_i = temperature at midpoint of element i in member section
T_1 = temperature at the bottom surface of section
T_2 = temperature at the top surface of section
T_1' = initial temperature at the bottom surface
T_2' = initial temperature at the top surface
x = distance from the bottom surface of section
y = distance from top fiber of section
ϵ_c = strain in the concrete
ϵ_{cr} = concrete cracking strain
ϵ_o = concrete strain at maximum compressive stress f_c'
ϵ_s = strain in the reinforcing/prestressing steel
$\bar{\epsilon}$ = strain at section's centroidal fiber under total load conditions
$\bar{\epsilon}'$ = strain at centroidal fiber due to unrestrained thermal load
$\bar{\epsilon}^\circ$ = strain at centroidal fiber under unloaded, unrestrained conditions
$\Delta\epsilon_p$ = locked-in prestressing strain
ϕ = section curvature under total load conditions
ϕ' = section curvature due to unrestrained thermal load
ϕ° = section curvature under unloaded, unrestrained conditions
Δ = elongation of member determined from joint deflections

REFERENCES

1. Priestley, M. J. N., "Thermal Stresses in Concrete Structures," *Proceedings,* Canadian Structural Concrete Conference, Toronto, 1981, pp. 255-283.

2. Thurston, S. J.; Priestley, M. J. N.; and Cooke, N., "Thermal Analysis of Thick Concrete Sections," ACI JOURNAL, *Proceedings* V. 77, No. 5, Sept.-Oct. 1980, pp. 347-357.

3. Thurston, S. J., "Thermal Stresses in Concrete Stresses," PhD thesis, *Research Report* No. 78-21, Department of Civil Engineering, University of Canterbury, Christchurch, 1978, 351 pp.

4. Priestley, M. J. N., "Design of Concrete Bridges for Temperature Gradients," ACI JOURNAL, *Proceedings* V. 75, No. 5, May 1978, pp. 209-217.

5. Freskakis, G. M., "Behavior of Reinforced Concrete at Elevated Temperatures," *Proceedings,* ASCE Specialty Conference on Civil Engineering and Nuclear Power (Knoxville, Sept. 1980), American Society of Civil Engineers, New York, V. 1, Paper No. 3-4.

6. Pajuhesh, Jim, "Thermal Relaxation in Concrete Structures," ACI JOURNAL, *Proceedings* V. 73, No. 9, Sept. 1976, 522-525.

7. Mentes, G. A.; Bhat, P. D.; and Ranni, A. I., "Thermal Effects in Reinforced Concrete Structures," *Proceedings,* ASCE Specialty Conference on Civil Engineering and Nuclear Power (Knoxville, Sept. 1980), American Society of Civil Engineers, New York, V. 1, Paper No. 3-5.

8. Kar, A. K., "Thermal Effects in Concrete Members," 4th Conference on Structural Mechanics in Reactor Technology, San Francisco, Aug. 1977, Paper J414, 11 pp.

9. ACI Committee 349, "Reinforced Concrete Design for Thermal Effects on Nuclear Power Plant Structures," (ACI 349.1R-80), American Concrete Institute, Detroit, 1980, 30 pp.

10. Gurfinkel, G., "Thermal Effects in Walls of Nuclear Containments—Elastic and Inelastic Behaviour," *Proceedings,* 1st Conference on Structural Mechanics in Reactor Technology (Berlin, 1971), V. 5-J, pp. 277-297.

11. Bhat, P. D., and Vecchio, F., "Design of Reinforced Concrete Containment Structures for Thermal Gradients Effects," 7th Conference on Structural Mechanics in Reactor Technology, Chicago, Aug. 1983, Paper J4/1, pp. 171-178.

12. Vecchio, F. J., "TEMPEST: A Computer Code for Nonlinear Structural Analysis of R/C Plane Frames," *Design of Structural Concrete,* Computer Publication COM-2(85), American Concrete Institute, Detroit, 1985, 120 pp.

13. Gere, J. M., and Weaver, W., *Matrix Analysis of Framed Structures,* D. Van Nostrand Co., New York, 1980, 492 pp.

14. Vecchio, Frank J., and Collins Michael P., "The Modified Compression-Field Theory for Reinforced Concrete Elements Subject to Shear," ACI JOURNAL, *Proceedings* V. 83, No. 2, Mar.-Apr. 1986, pp. 219-231.

APPENDIX — SECTION ANALYSIS ALGORITHM

Step 1 — Given: internal force resultants P and M and thermal gradient ΔT at time t for member. Discretize member section into m concrete layers and n reinforcing bar elements.

Step 2 — Compute temperature T_i at middepth of all components i ($i = 1, 2, \ldots, m + n$) using Eq. (11).

Step 3 — Compute thermal strain ϵ_{th} in all components

$$\epsilon_{th_i} = (T_i - T_i') \cdot \alpha$$

where α is the coefficient of thermal expansion and T_i' is the initial temperature in component i.

Step 4 — Compute creep strain ϵ_{crp} in all components based on previous stress conditions and elapsed time.

Step 5 — Estimate top and bottom fiber strain in section ϵ_{ct} and ϵ_{cb}.

Step 6 — Compute total strain ϵ_t in components

$$\epsilon_{t_i} = \epsilon_{ct} + (\epsilon_{cb} - \epsilon_{ct}) \cdot y_i/H$$

Step 7 — Compute stress-related strain ϵ in components

$$\epsilon_i = \epsilon_{t_i} - \epsilon_{th_i} - \epsilon_{crp_i}$$

Step 8 — Compute stress in each component using Eq. (3) through (10).

Step 9 — Evaluate resulting section forces P' and M' using Eq. (1) and (2).

Step 10 — Compare calculated force resultant P' and M' to given values P and M. If not equal, go to Step 5.

Step 11 — Compute section centroidal fiber strain $\bar{\epsilon}$ and curvature ϕ

$$\bar{\epsilon} = \epsilon_{ct} + (\epsilon_{cb} - \epsilon_{ct}) \cdot \bar{y}/H$$

$$\phi = (\epsilon_{cb} - \epsilon_{ct})/H$$

Note: The thermal strains in Step 3 need to be calculated only once.